Design of the target type flowmeter based on fiber Bragg grating and experiment

Xueguang Qiao (乔学光)[1], Qian Zhang (张 倩)[1,2], Haiwei Fu (傅海威)[1], and Dakuan Yu (禹大宽)[1]

[1]*Key Laboratory of Photoelectric Gas-Oil Logging and Detecting Ministry of Education, Xi'an Shiyou University, Xi'an 710065*
[2]*PetroChina Changqing Oilfield Company Communications Corporation, Xi'an 710018*

Received June 17, 2008

The target type flowmeter based on fiber Bragg gratings (FBGs) is experimentally studied. The relationship between the central wavelength shift of FBG and the flux is derived and the analytic expression is also given. Simulation and preliminary experiments have been carried out, and experimental validation of the water further proves the feasibility of the sensor. The experimental results verify the proposed sensor which can measure flux range from 200 to 1200 cm^3/s. And on this basis, the improvement program is raised.

OCIS codes: 060.3735, 280.0280.
doi: 10.3788/COL20080611.0815.

As in the oil industry, the measured fluid physical and chemical natures are complex. Only a relatively small number of flow sensors can be applied. Mechanical rotor flow sensor is widely used, but due to the mechanical structural constraints[1], it is of high measurement errors and low accuracy. Ultrasonic flow meter[2], electromagnetic, and acoustic Doppler current meter anemometers[3,4] have higher measurement accuracy and are more easily to be used, but the cost is high and they are vulnerable to electromagnetic interference. Fiber flow sensors have been developed in the last ten years[5,6]. Compared with other traditional flow sensors, fiber-optic flow sensors have many advantages, such as big dynamic measurement scope, thermostable high pressure, strong anti-electromagnetic interference ability, and so on[7−9].

This letter is based on the fiber Bragg grating (FBG) for sensing elements, the theoretical knowledge of hydrodynamics, and analysis of the velocity of the pressure generated by the target, using wavelength absolute encoder designs and new target FBG flow sensors. By changing the sensor material and size, the sensor can be passed to conduct a preliminary simulations experiments. This will be conducive to improving FBG flow sensor measurement sensitivity. More importantly, The sensor has done a verification experiment with water, giving further proof of the feasibility of the sensor.

The schematic diagram of the proposed the target type flowmeter based on FBGs is shown in Fig. 1. It consists of a target disc, a dowel steel, an isos-celes triangle cantilever, and a FBGs shown in Fig. 1(b). The cantilever is mounted on the pipe wall, perpendicular to the axis of the pipeline. The FBG is stuck along the centerline of the cantilever on one side. The force created by the fluid flow acts on the target disc and will be transferred to the cantilever by a dowel steel. The distortion of the cantilever then acts on the FBG, resulting in the wavelength shifts of the FBGs. Thus, when the cantilever is forced by the fluid flow, we have adopted a different cantilever to do a force experiment. Therefore we can find a relatively high sensitivity of the material and its structure.

If the average flow-rate of the fluid in pipeline is represented as V, the flow-rate at a random place within the pipeline can be described as

$$u(r) = 2 \cdot V \cdot \left[1 - \left(\frac{r}{R}\right)^2\right], \tag{1}$$

where R is the radius of the pipeline, r is the radial dimension from the center of the pipeline, as shown in Fig. 2.

On the assumption that the fluid is an ideal, incompressible steady flow, the whole mechanical energy at the place A and B is invariant. Thus, the kinetic energy of the fluid at the place A will be transformed into a pressure increment Δp, at the place B of the target disc, given by

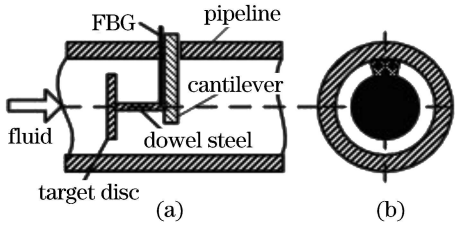

Fig. 1. Structure of the target type flowmeter based on FBG.

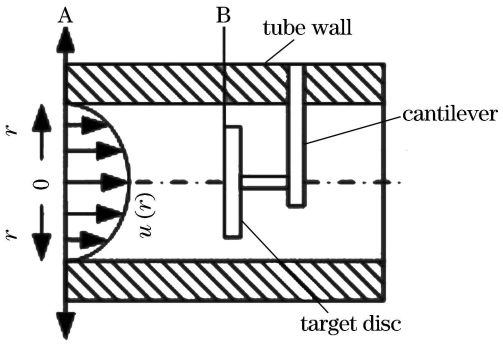

Fig. 2. Schematic of steady flow in a pipeline.

$$\Delta p = \frac{\rho \cdot u(r)^2}{2}, \tag{2}$$

where ρ is the fluid density.

Thus, the force acted on the target disc is given by $F = \oint_s \Delta p \cdot \mathrm{d}s$, where s is the limit of integration, that is, the area of the target disc, and $\mathrm{d}s$ is a micro surface element of integration on the target, which can be described as

$$\mathrm{d}s = \pi \cdot (r + \mathrm{d}r)^2 - \pi \cdot r^2 \approx 2\pi \cdot r \cdot \mathrm{d}r, \tag{3}$$

where r is the radial dimension from the center of the pipeline, as shown in Fig. 2, and $\mathrm{d}r$ is the micro radial increment with the target disc.

According to the above equations, the force acted on the target disc can be given by

$$F = \int_0^{d/2} \frac{\rho \cdot u(r)^2}{2} \cdot 2\pi \cdot r \cdot \mathrm{d}r$$

$$= \frac{\pi \cdot \rho \cdot V^2}{96R^4} \left(48R^4d^2 - 12R^2d^4 + d^6\right), \tag{4}$$

where d is the diameter of the target disc.

Based on the theory of material mechanics, the longitudinal strain on an isosceles triangle equalthickness cantilever can be expressed as the function of force applied at the free end of the cantilever by target disc, as shown in Fig. 1(b)

$$\varepsilon_x = \frac{6 \cdot F \cdot L}{E \cdot b_0 \cdot h^2}, \tag{5}$$

where L is the length and h is the thickness of cantilever, E is Youngs modulus of the cantilever material, b_0 is the width at the fixed end of the cantilever.

From Eq. (5), we can see that if the structural parameters are selected, the longitudinal strain on the isosceles triangle equal-thickness cantilever is independent on the positions, that is, the strain is constant along the cantilever, and is only a linear function of applied force. It is advantageous to avoid the chirped signals of grating spectrum and improve the resolution of wavelength-shift signals measurement.

Knowing the coupled mode theory, along with the FBG role of the axial stress (temperature remaining unchanged), the shift in Bragg wavelength $\Delta\lambda_\mathrm{B}$ with axial strain can be expressed[10] using

$$\Delta\lambda_\mathrm{B}/\lambda_\mathrm{B} = (1 - P_\mathrm{e})\,\varepsilon, \tag{6}$$

where $\varepsilon = \varepsilon_x$ is the applied strain, P_e is the photoelastic coeffcient of the fiber, for Ge-doped silica fiber, $P_\mathrm{e} = 0.22$.

The relation of the wavelength shift versus the average flow rate can be expressed based on Eqs. (4)—(6) as

$$\frac{\Delta\lambda_\mathrm{B}}{\lambda_\mathrm{B}} = (1 - P_\mathrm{e}) \frac{\pi \cdot L \cdot \rho \cdot V^2}{16E \cdot b_0 \cdot h^2 R^4}$$

$$\times \left(48R^4d^2 - 12R^2d^4 + d^6\right). \tag{7}$$

So, this volume flow can be calculated as $q_v = V \cdot \pi \left(R^2 - \frac{d^2}{4}\right)$.

To verify the feasibility of the proposed method and structures, preliminary experiments and simulations are carried out. The cantilever made from Maraging Steel is used with Youngs modulus $E_\mathrm{c} = 1.30 \times 10^5$ MPa, $h = 0.0009$ m, $b_0 = 0.006$ m, and $L = 0.04$ m being used. The FBG with $\lambda_\mathrm{B} = 1553.02$ nm, $P\mathrm{e} = 0.22$ is also used. On the assumption that the radius of the pipeline $R = 0.023$ m, the diameter of the target disc $d = 0.025$ m, and the density of the fluid $\rho = 1000$ kg/m^3, Fig. 3 shows the preliminary simulation experiment setup test the relation between wavelength shifts of FBG versus the applied force by target disc due to the flow-rate. Figure 4 shows the relation of the wavelength shift output of the sensor versus the flow variation through simulation experiment. It is based on the stress caused by wavelength drift, in accordance with the size of the force, by the use of the Eq. (4), calculating the average velocity. Further calculation is the size of the flow, which gives the relationship diagram that is the relationship of the fiber Bragg wavelength shift versus the flow variation. Figure 5 gives the spectrum of the wavelength shifts as the applied force increases. After having repeated stress tests, the sensor showed the stress response trend remaining basically unchanged. So the FBG on the stability of flow measurement is feasible.

After the simulation and preliminary experiments, the sensor was fixed to the flow measurement system, further validating the feasibility of the sensors. All the experimental parameters and the above parameters of the simulation were the same. Figure 6 shows the water flow through the valve controlling the size. When the water flow rate was stable, water was introduced from a small water tank which was on the electronic scale. From this moment, it was observed with a stopwatch, when electronic scale showed 10 to 14 kg, valves closed and records of time t and weight m. And through the spectrometer the center wavelength drift of the FBG was observed. From the use of experimental data above, volume flow was obtained, which is $q_v = m/\rho/t$. The sensor was made to repeat the experiment and the result was shown in Fig. 7 that the relation of the wavelength shift output of the sensor versus the flow variation through

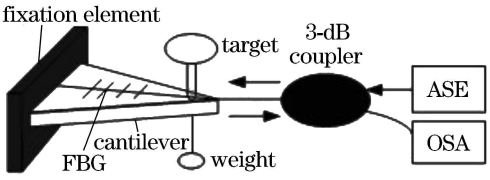

Fig. 3. Simulation experiment setup to test the relation between wavelength shifts of FBG and the applied force.

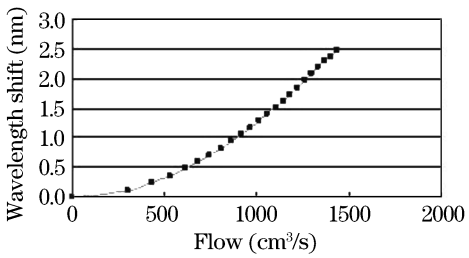

Fig. 4. Relation between the wavelength shift output of the sensor and the flow variation through simulation experiment.

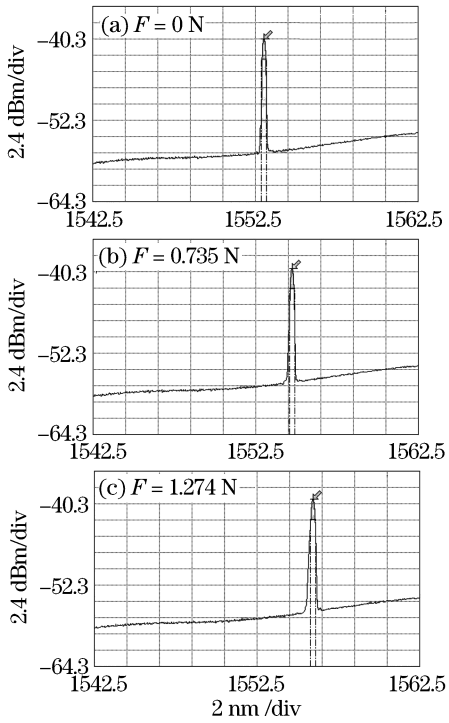

Fig. 5. Spectrum of the wavelength shifts as the applied force increases.

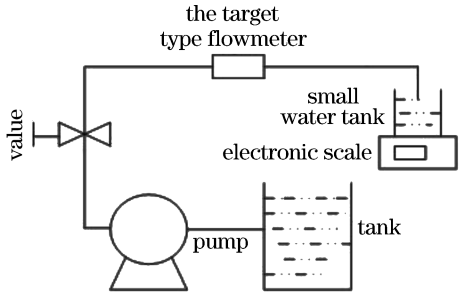

Fig. 6. Flow measurement system.

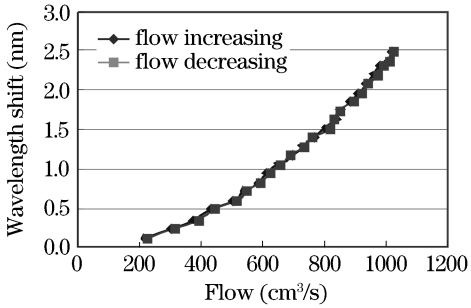

Fig. 7. Relation between the wavelength shift output of the sensor and the flow variation through experiment.

experimentation. The results showed that the sensor measurement repeatability was good.

In conclusion, based on the existing target type flowmeter, we proposed a new target FBG flow sensor. The experimental results indicated that this sensor could be used to measure the fluid flow with the flow-rate from 200 to 1200 cm^3/s. It compared well with the simulation results, with the existence of 90 to 300 cm^3/s error, but was basically the same with the shape of the curves. It can be seen from Fig. 7, the sensor measurement repeatability is very good, so through the repeated experiments with the average wavelength drift, we can calibrate the sensor.

Error is the cause of the target by the fluid in the shocks. The target of the plane and the cross-section of the pipeline have a certain angle, the greater velocity, the greater perspective, to a certain velocity of the target by the force than the formula calculated from theory. So drift in the same wavelength at the center of prague, the actual measurement of the flow of traffic than the simulation of small, experimental greater flow of traffic and simulation results compared with the greater error.

It was also possible to increase the sensor sensitivity and measurement range by changing the material and dimensions of the sensor structure. In addition, the presented measurement principles and the designed sensor structures also had advantages: 1) the sensor configuration consisted of non-electrical operation and no moving parts; 2) the measurement principle based on FBG light wavelength modulation avoided light intensity variation influence; 3) the designed isosceles triangle equal-thickness cantilever improved the quality of the FBG spectrum, resulting in the improvement of the measurement resolution.

In later experiments, two FBGs can be made to be symmetrically stuck along the centerline of the cantilever on either side. Through the dual-grating method[11], we can achieve the measurement distinction of fluid temperature and the flow rate.

This work was supported by the National "863" Project of China (No. 2006AA06Z210 and 2007AA03Z413), the National Natural Science Foundation of China (No. 60654001 and 60727004), and the Major Technological Innovation Program of Xi'an City of China (No. GG06004). Q. Zhang is the author to whom the correspondence should be addressed, her e-mail address is zhangqian214000@163.com.

References

1. L. Liang, Z. Chen, and Y. Wang, Process Automation Instrumentation (in Chinese) **24,** 41 (2003).
2. Y. Wang, X. Fu, Z. Li, and X. Hu, Acta Metrologica Sin. (in Chinese) **24,** 202 (2003).
3. X. Li, P. Wang, and J. Lu, Control and Instruments in Chemical Industry (in Chinese) **31,** 68 (2004).
4. Y. Xue, J. Gu, and T. Wei, Marine Sciences (in Chinese) **28,** 24 (2004).
5. J. Yao, J. Fu, C. Zhang, and X. Dong, Transducer Technology (in Chinese) **21,** 1 (2002).
6. J. Chen, W. Zhang, Q. Tu, Y. Zou, T. Zhao, X. Du, and X. Dong, Acta Opt. Sin. (in Chinese) **26,** 1136 (2006).
7. Q. Tu, W. Zhang, L. Sun, and X. Dong, Chinese J. Lasers (in Chinese) **31,** 1508 (2004).
8. W. Zhang, G. Kai, X. Dong, Y. Liu, W. Wang, and Z. Zhang, Acta Opt. Sin. (in Chinese) **24,** 330 (2004).
9. Q. Tu, W. Zhang, J. Chen, B. Liu, L. Jin, H. Niu, Z. Chen, and X. Dong, Acta Opt. Sin. (in Chinese) **25,** 1153 (2005).
10. Y. Zhang, D. Feng, and Z. Liu, IEEE Photon. Technol. Lett. **13,** 618 (2001).
11. X. Ye and T. Liu, Opto-Electron. Eng. **30,** (3) 23 (2003).